Possibility of a long-range proximity effect in a ferromagnetic nanoparticle

M. A. Silaev

Institute for Physics of Microstructures, Russian Academy of Sciences, GSP-105, 603950 Nizhny Novgorod, Russia

We study the proximity effect in a ferromagnetic nanoparticle having a vortex magnetization pattern. We show that for the axisymmetric system consisting of a circular particle and a magnetic vortex situated at the center of it no long-range superconducting correlations are induced. It means that induced superconductivity is localized in the small area near the superconducting electrode. However, in the real system axial symmetry can be broken by either a shift of the magnetic vortex from the origin or a geometrical anisotropy of the ferromagnetic particle. In this case a long-range proximity effect is possible.

I. INTRODUCTION

Proximity effect in hybrid ferromagnetic/superconducting (FS) structures reveals a rich physics originating from the interplay between magnetic and superconducting types of ordering (see Ref. 1 for review). There are two essential features of the proximity effect in FS structures which make it different from that in superconductor/normal-metal (SN) structures. In SN structures the penetration length of a condensate wave function into the normal metal is determined by the normal-metal coherence length $\xi_N = \sqrt{D/2\pi T}$, where D and T are the diffusion coefficient and temperature. First, in contrast a ferromagnetic coherence length which is also a depth of the condensate penetration into a ferromagnet in FS system is much shorter $\xi_F = \sqrt{D/h}$ provided that the exchange energy h is rather large $h \gg T$ which is usually fulfilled. Second, the penetration of Cooper pair wave function into the ferromagnetic region (F) is characterized by the damped oscillatory behavior of a correlation function $f \sim \exp(-x/\xi_F)\sin(x/\xi_F)$ which is a result of exchange splitting between energy bands of conduction electrons with different spin projections. In fact the origin of oscillations is the same as for the Fulde-Ferrel-Larkin-Ovchinnikov state.[2] This results in many new effects, such us spatial oscillations of the density of states,[3] a nonmonotonic[4] or reentrant[5] behavior of the critical temperature as a function of a ferromagnetic layer thickness in layered FS structures. Also it is responsible for the formation of Josephson π junctions[6] and spin valves.[7]

Despite the short coherence length in the ferromagnetic region there is a possibility of a long-range proximity effect in FS structures with inhomogeneous magnetic structure. In experiments on FS systems with strong ferromagnets an anomalously large increase in the conductance below the superconducting critical temperature T_c was observed.[8–10] Also recently the Andreev interferometer geometry was used to measure the phase sensitive conductance modulation in the FS system with helical magnetic structure.[11]

The first theoretical analysis of a long-range proximity effect in FS structure with inhomogeneous magnetization was done for a Bloch-type domain wall at the FS interface.[12] It was shown that a superconducting correlation function contains components which survive at the distances of order of the normal-metal correlation length from the superconducting boundary. These long-range superconducting components have nontrivial structure in spin space. Conversely to the ordinary Cooper pairs which have a singlet spin structure they have a triplet spin structure which corresponds to correlations between electrons with the same spin projections. Therefore the long-range superconducting components in FS systems are usually called the long-range triplet components (LRTC). The LRTC can be generated in systems with Bloch[12] and Neel[13,14] domain walls or helical magnetization pattern.[15] The long-range proximity effect was shown to exist in multilayered FS structures with noncollinear magnetization in different ferromagnetic layers.[16–19] Large attention has been paid to the investigation of long-range Josephson effect due to LRTC in FS systems (see Ref. 20 for a review). Recently in Ref. 19 a multilayered *SFIFIFS* structure has been shown to demonstrate a controllable crossover between long-range triplet and short-range singlet Josephson effects with the rotation of the magnetic moment of any of the F layers.

The present paper is devoted to another possibility of controllable switching between long- and short-range proximity effects by employing the peculiar properties of ferromagnetic nanoparticles. In some sense the magnetization of a nanoparticle is more simple than the domain structure of macroscopic ferromagnets; therefore, theoretical findings could be proven by experiments with nanoparticles. It is now well understood that a magnetization distribution in a single particle is determined by the competition between the magnetostatic and exchange energies. If a particle is small, it is uniformly magnetized, and if its size is large enough a nonuniform (vortex) magnetization is more energy preferable (see, for example, Refs. 21–28). Besides the geometrical form and size, the state of the particle depends on many other factors. For example, if the ferromagnetic particle is initially in the vortex state then by applying a homogeneous in-plane magnetic field one can shift the center of a magnetic vortex toward the particle edges.[29] If the magnetic field is large enough the magnetic vortex annihilates; i.e., the particle becomes homogeneously magnetized. Conversely, by applying magnetic field to the homogeneously magnetized particle in the direction opposite to its magnetic moment one can force a nucleation of magnetic vortex. Experimentally the shifting of magnetic vortex is observed as a linear growth of the particle magnetic moment which saturates at the field of vortex annihilation. A transition from homogeneous to vortex state leads to a large jump of the magnetic moment so
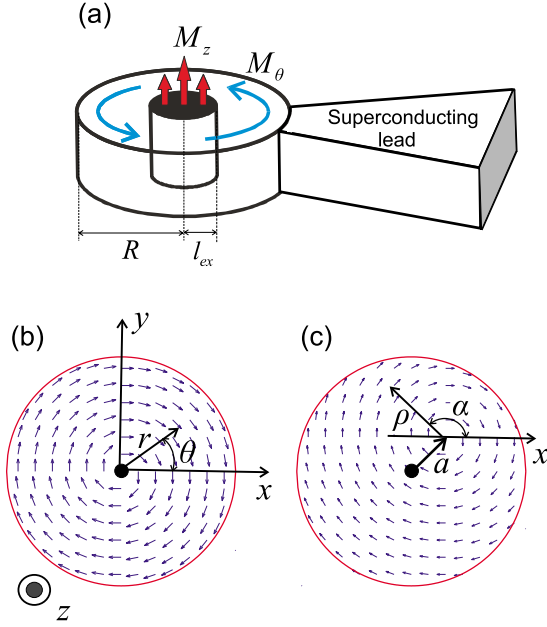
FIG. 1. (Color online) Sketch of the system considered: (a) ferromagnetic nanoparticle with vortex magnetization and attached superconducting electrode. (b) Magnetic vortex at the center of the circular particle and the polar coordinate system. (c) Shifted magnetic vortex and the polar coordinate system with the origin at the vortex center.

the magnetization curve of a ferromagnetic nanoparticle is in general highly hysteretic.[30]

In practice superconducting correlations in a ferromagnetic nanoparticle can be induced in planar geometry by lateral superconducting junctions connected to the particle. Obviously if the particle is homogeneously magnetized then no long-range correlations are induced and the proximity effect is short range. If the particle is in vortex state the situation is not so obvious and the special investigation is needed. Throughout this paper we will consider only the vortex state of the ferromagnetic particle. We will show that for a circular particle there is no long-range superconducting correlations if the magnetic vortex is situated at the center. However if the magnetic vortex is shifted from the center by an external field there appear long-range correlations. Moreover an axial anisotropy of geometric form of the particle also leads to a long-range proximity effect.

The structure of this paper is as follows. In the next section we describe our model, present the basic equations, and give a qualitative explanation of the long-range proximity effect in a ferromagnetic nanoparticle with vortex magnetization. In Sec. IV we present our main results which are discussed in Sec. V. Finally the conclusions are given in Sec. VI.

II. MODEL AND BASIC EQUATIONS

We consider a system shown schematically in Fig. 1. It consists of a ferromagnetic nanoparticle and a lateral superconducting lead. The particle magnetization is assumed to form a magnetic vortex state. The structure of magnetic vor-

tex is shown in Fig. 1(b). It can be described by the rigid vortex model proposed by Usov and Peschany[31] and by Guslienko and co-workers.[29] Within this model magnetization has a z component only inside the core region whose size is determined by a ferromagnetic exchange length l_{ex}. Outside this region magnetization lies within xy plane. Typically the exchange length is quite small $l_{ex} \sim 10$ nm compared to the sizes of ferromagnetic nanoparticles $R \sim 100$ nm; therefore, we will neglect the vortex core region throughout this paper. Thus if the center of magnetic vortex is situated at the point $\mathbf{r} = \mathbf{a}$ the magnetization distribution can be written in the following form:

$$\mathbf{M} = q_m M_0 [\mathbf{n}_\rho, \mathbf{z_0}], \tag{1}$$

where $\mathbf{z_0}$ is a unit vector along the z axis, $\mathbf{n}_\rho = (\mathbf{r} - \mathbf{a})/|\mathbf{r} - \mathbf{a}|$ and $\mathbf{a}$ is a shifting vector of magnetic vortex center with respect to the origin. In polar coordinate system (ρ, α) with the origin at the center of magnetic vortex [see Fig. 1(c)] magnetization distribution (1) takes a simple form as follows:

$$\mathbf{M} = q_m M_0 (\sin \alpha, -\cos \alpha). \tag{2}$$

Equation (2) describes the magnetization vector curling around the center $\mathbf{r} = \mathbf{a}$ in a clockwise (counterclockwise) direction for $q_m = +1(-1)$. Further we will assume a clockwise direction of magnetization rotation [see Fig. 1(b)]. Note that in case of a circular ferromagnetic particle the shift of a magnetic vortex from the center can be directly related to the external magnetic field $\mathbf{H}_{ext}$ as follows:

$$\mathbf{a} = \chi_p \frac{\mathbf{z_0} \times \mathbf{H}}{M_0}, \tag{3}$$

where χ_p is the ferromagnetic nanoparticle linear magnetic susceptibility.[29] The corresponding distribution of the effective exchange field acting on free electrons can be taken as $\mathbf{h} = h_0 \mathbf{M}/M_0$, where h_0 is determined by the value of the exchange integral (see, e.g., Ref. 1).

Our goal is to find a condensate Green's function in the ferromagnetic particle induced by an attached superconducting lead due to a proximity effect [see Fig. 1(a)]. We consider the "dirty limit" assuming that the mean-free path of electrons is much shorter than all coherence lengths: $l \ll \xi_s, \xi_N, \xi_F$. The most restrictive condition is $l \ll \xi_F$ since the ferromagnetic coherence length is much shorter than coherence lengths in superconductor ξ_s and normal metal ξ_N. It imposes certain limitation on the magnitude of exchange interaction which means that the ferromagnetic should not be very "strong."

To analyze a proximity effect in ferromagnetic particle we will use Usadel equations for quasiclassical Green's functions. Following the scheme presented in detail in review[20] we introduce a matrix Green's function,[32]

$$\check{g} = \begin{pmatrix} \hat{g} & \hat{f} \\ \hat{f}^+ & \bar{\hat{g}} \end{pmatrix}.$$

Here $\hat{g}$ is normal and $\hat{f}$ is anomalous Green's functions which are matrices in spin space. A space where the matrix $\check{g}$ is

defined is a Gor'kov-Nambu space. We will denote Pauli matrices in Gor'kov-Nambu space as $\hat{\tau}_i$ and in spin space as $\hat{\sigma}_i$ ($i=1,2,3$). Unit matrices are $\hat{\tau}_0$ and $\hat{\sigma}_0$, respectively. Following Ref. 20 the spinor basis for Green's functions is taken in the following form:

$$\hat{g} = \begin{pmatrix} \uparrow\uparrow & \uparrow\downarrow \\ \downarrow\uparrow & \downarrow\downarrow \end{pmatrix},$$

$$\hat{f} = \begin{pmatrix} \uparrow\downarrow & \uparrow\uparrow \\ \downarrow\downarrow & \downarrow\uparrow \end{pmatrix},$$

where $\uparrow$ and $\downarrow$ denote the spinors corresponding to spin projections $s_z = \pm 1/2$.

It is convenient to use a transformation of Green's function $\check{g}$ suggested by Ivanov and Fominov[33] $\check{g} = \check{V}\check{g}_{\text{new}}\check{V}^+$, where

$$\check{V} = \exp\left[-i\frac{\pi}{4}(\hat{\tau}_3 - \hat{\tau}_0)\hat{\sigma}_3 \right]. \quad (4)$$

After this transformation is done the Usadel equation for the matrix Green's function $\check{g}$ takes the following form:

$$D\,\nabla\,(\check{g}\,\nabla\,\check{g}) - \omega[\hat{\tau}_3, \check{g}] - i[\hat{\tau}_3(\mathbf{h}\cdot\hat{\sigma}), \check{g}] - [\check{\Delta}, \check{g}] = 0, \quad (5)$$

where [..] is a commutator, D is a diffusion coefficient, ω is Matsubara frequency, and $\mathbf{h} = (h_x, h_y, h_z)$ is an effective exchange field. The gap function is given by

$$\check{\Delta} = (\hat{\tau}_1 \text{ Im } \Delta - \hat{\tau}_2 \text{ Re } \Delta)\hat{\sigma}_0.$$

If there are no superconducting correlations in the normal-metal region then the Green's function (in Matsubara representation) is given by

$$\check{g}(\omega) = \text{sgn}(\omega)\hat{\tau}_3\hat{\sigma}_0. \quad (6)$$

Equation (5) can be linearized assuming that

$$\check{g} = \text{sgn}(\omega)\hat{\tau}_3\hat{\sigma}_0 + \check{F}, \quad (7)$$

where second term is small $|\check{F}| \ll 1$. Then we obtain a linearized equation for $\check{F}$ as follows:

$$D\nabla^2\check{F} - 2|\omega|\check{F} - i\,\text{sgn}(\omega)\{\hat{\tau}_0(\mathbf{h}\cdot\hat{\sigma}), \check{F}\} = 0, \quad (8)$$

where {..} is anticommutator. The linearized boundary condition for the function $\check{F}$ at the S/F interface is

$$\mathbf{n}\cdot\nabla\check{F} = \check{F}_S/\gamma, \quad (9)$$

where $\gamma = R_b\sigma$, where R_b is the interface resistance per unit area and σ is the conductivity of the ferromagnet; $\mathbf{n}$ is a unit vector normal to boundary. The anomalous function in bulk superconductor is

$$\check{F}_S = (\hat{\tau}_1 \sin\varphi - \hat{\tau}_2 \cos\varphi)\hat{\sigma}_0 F_{\text{bcs}}.$$

Here $F_{\text{bcs}} = \Delta_0/\sqrt{\Delta_0^2 + \omega^2}$, where φ and Δ_0 are the phase and module of the superconducting order parameter.

Note that in Eq. (8) the components of $\check{F}$ proportional to $\hat{\tau}_1$ and $\hat{\tau}_2$ are not coupled to each other. Thus in ferromag-

netic region anomalous function has the following structure: $\check{F} = (\hat{\tau}_1 \sin\varphi - \hat{\tau}_2 \cos\varphi)\hat{f}$, where $\hat{f}$ is a matrix in spin space. For the function $\hat{f}$ (when matrices in Nambu space are omitted) we obtain the following equation in ferromagnetic region:

$$D\nabla^2\hat{f} - 2|\omega|\hat{f} - i\text{sgn}(\omega)\mathbf{h}\cdot\{\hat{\sigma}, \hat{f}\} = 0. \quad (10)$$

The solution of Eq. (10) can be found as a superposition as follows:

$$\hat{f} = a_0\hat{\sigma}_0 + a_1\hat{\sigma}_1 + a_2\hat{\sigma}_2 + a_3\hat{\sigma}_3. \quad (11)$$

In this expansion the first term corresponds to the singlet component and the last three terms correspond to the triplet components of anomalous function with different directions of Cooper pair spin. Note that after transformation (4) the spin space basis for the anomalous function $\hat{f}$ can be symbolically written as follows:

$$\hat{f} = \begin{pmatrix} \uparrow\downarrow & -\uparrow\uparrow \\ \downarrow\downarrow & -\downarrow\uparrow \end{pmatrix}.$$

Therefore it can be seen that

$$\hat{S}_i\hat{\sigma}_i = 0,$$

where $\hat{S}_i$ is an operator of spin projection for a Cooper pair with respect to the ith axis ($i = x, y, z$). If the vector $\mathbf{f}_{\text{tr}} = (a_1, a_2, a_3)$ is parallel to some real vector $\mathbf{q}$ in $3D$ space then the Cooper pair spin projection on the vector $\mathbf{q}$ is zero. This means that the Cooper pairs consist of electrons with the opposite spin projections, or in other worlds the spin lies in the plane perpendicular to vector $\mathbf{q}$. As we will see below the exchange field $\mathbf{h}$ collinear with the vector $\mathbf{q}$ effectively decouples the electrons leading to the fast decay of Cooper pair wave function into the ferromagnetic region. Otherwise if the vector $\mathbf{q}$ (or more generally $\mathbf{f}_{\text{tr}}$) is not collinear to exchange field $\mathbf{h}$ the LRTC appears.

The equations for coefficients a_i are as follows:

$$D\nabla^2a_0 - 2|\omega|a_0 - i\,\text{sgn}(\omega)\mathbf{h}\cdot\mathbf{f}_{\text{tr}} = 0, \quad (12)$$

$$D\nabla^2a_1 - 2|\omega|a_1 - i\,\text{sgn}(\omega)h_xa_0 = 0, \quad (13)$$

$$D\nabla^2a_2 - 2|\omega|a_2 - i\,\text{sgn}(\omega)h_ya_0 = 0, \quad (14)$$

$$D\nabla^2a_3 - 2|\omega|a_3 - i\,\text{sgn}(\omega)h_za_0 = 0. \quad (15)$$

Now let us discuss the general structure of solutions of Eqs. (12)–(15). If the magnetization and thus exchange field are homogeneous then it is easy to see that there are two types of solutions of Eqs. (12)–(15): (i) short-range and (ii) long-range modes. Indeed if the vector $\mathbf{f}_{\text{tr}} = (a_1, a_2, a_3)$ is parallel to the vector $\mathbf{h}$ then we obtain two equations for the functions a_0 and $b = |\mathbf{f}_{\text{tr}}|$ as follows:

$$D\nabla^2a_0 - 2|\omega|a_0 - i\,\text{sgn}(\omega)hb = 0, \quad (16)$$

$$D\nabla^2 b - 2|\omega|b - i\,\text{sgn}(\omega)ha_0 = 0, \qquad (17)$$

which have solutions in the form: $(a_0, b) \sim \exp(\lambda \mathbf{n} \cdot \mathbf{r})$, where $\lambda = \pm(1 \pm i)k_h/\sqrt{2}$ and $k_h = 1/\xi_F = \sqrt{h/D}$ and $\mathbf{n}$ is a unit vector with arbitrary direction. These modes are short-range ones since ferromagnetic exchange length ξ_F is typically very short. One can see that short-range modes consist of the singlet part of the anomalous function with the amplitude given by coefficient a_0. Also it is a nonzero contribution from triplet parts. The Cooper pair spin is directed perpendicular to the exchange field $\mathbf{h}$. Therefore, such triplet superconducting correlations are suppressed by the exchange field on the same length scale as the singlet ones.

On the other hand if the vector $\mathbf{f}_{\text{tr}}$ is perpendicular to $\mathbf{h}$ then the Cooper pair spin can be oriented along $\mathbf{h}$. In this case the destructive influence of exchange field on Cooper pairs is reduced. Indeed, from Eqs. (12)–(15) we obtain that $a_0 = 0$ and b satisfies the following equation:

$$D\nabla^2 b - 2|\omega|b = 0, \qquad (18)$$

which have a solution $b \sim \exp(\lambda \mathbf{n} \cdot \mathbf{r})$, where $\lambda = \pm 1/\xi_N$ and $\xi_N = \sqrt{D/|\omega|}$. These modes are long-range ones because the coherence length in normal metal ξ_N can be rather large. Note that since $a_0 = 0$ these modes contain no singlet component; i.e., they contain only LRTC.

In case of homogeneous magnetization long-range modes cannot be excited because of the zero boundary conditions for the triplet components,

$$\mathbf{n} \cdot \nabla a_i = 0, \qquad (19)$$

for $i = (1, 2, 3)$. The sources at the FS boundary exist only for a singlet component,

$$\mathbf{n} \cdot \nabla a_0 = F_{\text{bcs}}/\gamma, \qquad (20)$$

where $\mathbf{n}$ is a unit vector normal to the boundary. However it is not so for the inhomogeneous magnetization distribution. The well-known examples when LRTC can be excited are Bloch domain wall in a thin ferromagnetic wire[12] or spiral magnetic structure which can be realized in some rare-earth metals.[15] Also recently the case of Neel domain walls in planar proximity FS structure was investigated.[13,14]

Now let us consider magnetic structure with large scale inhomogeneities. In zero-order approximation for short-range modes we obtain Eqs. (16) and (17) for a_0 and $b = |\mathbf{f}_{\text{tr}}|$ again, although the direction of vector $\mathbf{a}$ adiabatically depends on the coordinate: $\mathbf{f}_{\text{tr}} = b\mathbf{h}/h$. The solution can be written in the following form: $(a_0, b) = (A, B)F(\mathbf{r})$, where A and $B = A(k_h/\lambda)^2$ are constant and $F(\mathbf{r}) = \exp(\lambda \cdot \mathbf{r})$. Boundary conditions (19) and (20) can be written as follows:

$$\mathbf{n} \cdot \nabla a_0 = F_{\text{bcs}}/\gamma, \qquad (21)$$

$$\mathbf{h}(\mathbf{n} \cdot \nabla b) = -b\,(\mathbf{n} \cdot \nabla)\mathbf{h}, \qquad (22)$$

where $\mathbf{n}$ is a unit vector normal to the boundary. There are two short-range modes which decay far from FS boundary in the ferromagnetic region, say, with $\lambda_1 = k_h(1+i)/\sqrt{2}$ and $\lambda_2 = k_h(1-i)/\sqrt{2}$. Taking the superposition of these modes with arbitrary coefficients A_1 and A_2 we obtain from Eq. (22),

$$A_1(\lambda_1 - S_1) + A_2(\lambda_2 - S_2) = 0,$$

$$A_1(\lambda_1 - S_2) + A_2(\lambda_2 - S_1) = 0,$$

where $S_1 = (\mathbf{n} \cdot \nabla)h_x/h$ and $S_2 = (\mathbf{n} \cdot \nabla)h_y/h$. This linear system of the homogeneous equations has a solution if and only if $S_1 = S_2$; i.e.,

$$(\mathbf{n} \cdot \nabla)h_x = (\mathbf{n} \cdot \nabla)h_y. \qquad (23)$$

This condition is fulfilled only in some special cases. The most trivial of them is a homogeneous magnetization distribution. Another particular case when condition (23) is fulfilled is that of a circular ferromagnetic particle if the magnetic vortex is situated at the center of the particle. Indeed in this case $h_{x,y}$ depend only on θ and therefore $(\mathbf{n} \cdot \nabla)h_{x,y} = (\partial/\partial r)h_{x,y} = 0$. Otherwise if the magnetic vortex is shifted from the center or the particle shape is axially symmetric condition (23) is not fulfilled. It means that taking into account the short-range modes only one cannot satisfy the boundary conditions and with necessity the long-range modes are excited.

The above qualitative description of the eigenmode structure is based on the assumption of adiabatically slow variation in magnetization and exchange field $\mathbf{h}$. On the other hand in boundary condition (22) appears a derivative of $\mathbf{h}$ which in fact is a source for long-range modes. Below we will find the corrections to the above adiabatic structure of short-range modes. We will show that even if these corrections are taken into account it is still not possible to satisfy boundary condition (22) considering only the short-range modes.

III. STRUCTURE OF SHORT- AND LONG-RANGE MODES IN MAGNETIC VORTEX

For further considerations it is convenient to introduce functions $b_{\pm} = a_1 \pm ia_2$. Taking the magnetization distribution in form (2) we obtain

$$(\nabla^2 - k_\omega^2)a_0 - i\frac{k_h^2}{2}\text{sgn}(\omega)[S^*(\mathbf{r})b_+ + S(\mathbf{r})b_-] = 0, \quad (24)$$

$$(\nabla^2 - k_\omega^2)b_+ - i\,\text{sgn}(\omega)k_h^2 S(\mathbf{r})a_0 = 0, \qquad (25)$$

$$(\nabla^2 - k_\omega^2)b_- - i\,\text{sgn}(\omega)k_h^2 S^*(\mathbf{r})a_0 = 0, \qquad (26)$$

where $k_\omega^2 = 2|\omega|/D$ and $k_h^2 = h_0/D$. We have introduced the following function: $S(\mathbf{r}) = (h_x + ih_y)/h_0$, where $h_0 = \sqrt{h_x^2 + h_y^2}$.

A. Short-range modes

Usually the ferromagnetic coherence length $\xi_F = 1/k_h$ is very short. Most importantly it is much smaller than the size of a particle R and the characteristic scale of the magnetization distribution given by the function $S(\mathbf{r})$. Therefore solutions of Eqs. (24)–(26) with effective wavelength ξ_F can be described within quasiclassical approximation. Also we neglect terms proportional to k_ω^2. Physically it is justified since usually the normal-metal coherence length $\xi_N \sim 1/k_\omega$ is

much larger than the ferromagnetic coherence length ξ_F.

Then we obtain the solution of Eqs. (24)–(26) in the following form (see Appendix A for details):

$$a_0 = F(\theta)\exp(\lambda \mathbf{n} \cdot \mathbf{r}), \qquad (27)$$

$$b_+ = iF(\theta)\operatorname{sgn}(\omega)\exp(\lambda \mathbf{n} \cdot \mathbf{r})\frac{k_h^2}{\lambda^2}\left[1 - \frac{2}{\lambda}(\mathbf{n} \cdot \nabla)\right]S, \quad (28)$$

$$b_- = iF(\theta)\operatorname{sgn}(\omega)\exp(\lambda \mathbf{n} \cdot \mathbf{r})\frac{k_h^2}{\lambda^2}\left[1 - \frac{2}{\lambda}(\mathbf{n} \cdot \nabla)\right]S^*, \quad (29)$$

where $F(\theta)$ is an arbitrary 2π periodic function and $\lambda = \lambda_{1,2} = k_h(1 \pm i)/\sqrt{2}$.

B. Long-range modes

Now we are going to consider slow modes of Eqs. (24)–(26). For this purpose we choose the coordinate origin at the magnetic vortex center (ρ, α) [see Fig. 1(c)]. Then we have $S(\mathbf{r}) = -ie^{i\alpha}$, and therefore Eqs. (24)–(26) allow separation of variables: $a_0 = a_{\rho0}(\rho)e^{iM\alpha}$, $b_+ = b_{\rho+}(\rho)e^{i(M+1)\alpha}$, and $b_- = b_{\rho-}(\rho)e^{i(M-1)\alpha}$. Then we obtain the following:

$$\left[\frac{1}{\rho}\frac{\partial}{\partial\rho}\left(\rho\frac{\partial}{\partial\rho}\right) - \frac{M^2}{\rho^2} - k_\omega^2\right]a_{\rho0} - \operatorname{sgn}(\omega)\frac{k_h^2}{2}(b_{\rho-} - b_{\rho+}) = 0, \qquad (30)$$

$$\left[\frac{1}{\rho}\frac{\partial}{\partial\rho}\left(\rho\frac{\partial}{\partial\rho}\right) - \frac{(M+1)^2}{\rho^2} - k_\omega^2\right]b_{\rho+} - \operatorname{sgn}(\omega)k_h^2 a_{\rho0} = 0, \qquad (31)$$

$$\left[\frac{1}{\rho}\frac{\partial}{\partial\rho}\left(\rho\frac{\partial}{\partial\rho}\right) - \frac{(M-1)^2}{\rho^2} - k_\omega^2\right]b_{\rho-} + \operatorname{sgn}(\omega)k_h^2 a_{\rho0} = 0. \qquad (32)$$

The behavior of solutions of Eqs. (30)–(32) depends on the ratio of the ferromagnetic particle size and normal-metal coherence length R/ξ_N. Indeed if $R \gg \xi_N$ these modes decay at the length ξ_N. This is not very interesting case both for the experiment and for the theoretical study. Another limit which can be investigated analytically is realized when $\xi_N \gg R$. It means that the decay of the long-range modes on the size of a ferromagnetic particle is weak. This condition is the most favorable for investigation of the long-range proximity effect. Therefore we neglect terms proportional to k_ω^2 from Eqs. (30)–(32).

It is possible to find the long-range modes as expansion by the orders of small parameter $(Rk_h)^{-1}$. The details of the calculations are shown in Appendix B. We obtain the following solution: $a_{\rho0} = 0$,

$$b_{\rho+} = b_{\rho-} = B\rho^{\sqrt{M^2+1}}, \qquad (33)$$

where B is an arbitrary coefficient.

IV. RESULTS

We will find the distribution of anomalous Gor'kov function in a ferromagnetic nanoparticle induced by a supercon-

ducting electrode which is attached to the particle as it is shown in Fig. 1. The superconducting electrode attached at some point to the ferromagnetic sample can be modeled by the angle-dependent transparency of the FS interface $\gamma = \gamma(\theta)$ in boundary condition (20). For simplicity we can consider a Gauss form of transparency,

$$\gamma = \gamma_0 \exp\left\{-\frac{[(\theta - \theta_0)\operatorname{mod} 2\pi]^2}{\delta\theta^2}\right\}, \qquad (34)$$

where $\delta\theta$ is determined by a junction width $d = R(\delta\theta/2\pi)$.

Let us start with a general consideration. The boundary conditions for the coefficients a_0, b_+, and b_- at the boundary of a ferromagnetic particle read as follows:

$$\mathbf{n} \cdot \nabla a_0 = \frac{F_{\text{bcs}}}{\gamma(\theta)}, \qquad (35)$$

$$\mathbf{n} \cdot \nabla b_{\pm} = 0. \qquad (36)$$

To satisfy the boundary condition for a_0 we take the superposition of solutions (27)–(29) corresponding to $\lambda_1 = k_h(1+i)/\sqrt{2}$ and $\lambda_1 = k_h(1-i)/\sqrt{2}$ with arbitrary functions $F_{1,2}(\theta)$. We will take into account only those solutions which decay far from the FS boundary. Using expression (2) for the vortex magnetization and taking into account that $S(\mathbf{r}) = -ie^{i\alpha}$ from Eqs. (35) and (36) we obtain as follows:

$$\sum_{j=1,2}\lambda_j F_j(\theta) = \frac{F_{\text{bcs}}}{\gamma}, \qquad (37)$$

$$e^{i\alpha}\operatorname{sgn}(\omega)\sum_{j=1,2}F_j(\theta)\frac{k_h^2}{\lambda_j}\left[1 - \frac{i}{\lambda_j}(\mathbf{n} \cdot \nabla\alpha)\right] + \mathbf{n} \cdot \nabla b_{l+} = 0, \qquad (38)$$

$$e^{-i\alpha}\operatorname{sgn}(\omega)\sum_{j=1,2}F_j(\theta)\frac{k_h^2}{\lambda_j}\left[1 + \frac{i}{\lambda_j}(\mathbf{n} \cdot \nabla\alpha)\right] - \mathbf{n} \cdot \nabla b_{l-} = 0, \qquad (39)$$

where $b_{l\pm}(\mathbf{r})$ are the contributions of the long-range modes. The structure of the long-range modes yields the following relation for the coefficients $e^{-i\alpha}b_{l+} = e^{i\alpha}b_{l-}$. Let us denote $\operatorname{sgn}(\omega)b_{l0} = e^{-i\alpha}b_{l+} = e^{i\alpha}b_{l-}$. Then from Eqs. (38) and (39) we obtain as follows:

$$\frac{F_1}{\lambda_1} + \frac{F_2}{\lambda_2} = -ib_{l0}\frac{\mathbf{n} \cdot \nabla\alpha}{k_h^2}, \qquad (40)$$

$$(\mathbf{n} \cdot \nabla\alpha)\left(\frac{F_1}{\lambda_1^2} + \frac{F_2}{\lambda_2^2}\right) = i\frac{\mathbf{n} \cdot \nabla b_{l0}}{k_h^2}. \qquad (41)$$

One has $\lambda_{1,2} \sim k_h$; therefore, the r.h.s. of Eq. (40) is small and with good accuracy $F_1/\lambda_1 + F_2/\lambda_2 = 0$. Equations (37) and (41) then yield

$$F_{1,2} = F_{\text{bcs}}/(2\gamma\lambda_{1,2}) \qquad (42)$$

and

$$\mathbf{n} \cdot \nabla b_{l0} = \frac{i}{\sqrt{2}k_h}\frac{F_{\text{bcs}}}{\gamma}(\mathbf{n} \cdot \nabla\alpha), \qquad (43)$$

We search the contribution from the long-range modes as a superposition,

$$b_{l0} = \sum C_m \rho^{\sqrt{m^2+1}} e^{im\alpha}, \tag{44}$$

where ρ, α are the polar coordinates relative to the center of a magnetic vortex. We use numerical methods to calculate the coefficients in sum (44). We assume the angle-dependent transparency in Eq. (35) in form (34) with $\delta\theta = 0.02$ and the value of the ferromagnetic coherence length $\xi_F = 0.02R$. Further we will consider two typical cases: (i) magnetic vortex in a circular particle shifted from the center of it and (ii) magnetic vortex at the center of a particle having the elliptical shape.

A. Shifted magnetic vortex

Let us assume for simplicity that the shifting vector is directed along the x axis: $\mathbf{a} = (a_x, 0)$. The vector normal to the boundary is directed along the disk radius: $\mathbf{n} = \mathbf{r}/r$. Then the short-range modes are given by Eqs. (27)–(29) with

$$S(\mathbf{r}) = \frac{i(a - re^{i\theta})}{(r^2 - 2ar\cos\theta + a^2)^{1/2}}$$

and

$$(\mathbf{n} \cdot \nabla)S = \frac{dS}{dr} = \frac{a\sin\theta(a - re^{i\theta})}{(r^2 - 2ar\cos\theta + a^2)^{3/2}}.$$

The boundary condition for the long-range modes [Eq. (43)] takes the following form:

$$\left.\frac{db_{l0}}{dr}\right|_{r=R} = \frac{i}{\sqrt{2}k_h}\frac{F_{\text{bcs}}}{\gamma}Q(\theta), \tag{45}$$

where

$$Q(\theta) = \frac{a\sin\theta}{(R^2 - 2aR\cos\theta + a^2)}.$$

In general, the amplitudes of the short-range modes given by Eqs. (27) and (42) are determined by the dimensionless factor ξ_F/γ_0. From Eq. (33) it is easy to see that $db_{l0}/dr(r = R) \sim b_{l0}/R$. Thus, when the vortex shifting is small ($a \ll R$) the amplitude of LRTC is determined by the dimensionless factor $(\xi_F/\gamma_0)(a/R)$; i.e., it is (R/a) times smaller than the amplitudes of the short-range triplet components.

In case when a junction with a superconducting lead is narrow $\delta\theta \ll 2\pi$, the amplitude of the LRTC is determined by the function $|Q(\theta_0)|$. One can see that the maximum amplitude is obtained when $\cos\theta_0 = 2aR/(R^2 + a^2)$. On the other hand the long-range proximity effect is absent if $\theta_0 = 0$ or π. This is caused by the symmetry of the magnetization distribution. In such case the magnetization is constant along the direction of surface normal vector at the point where the superconducting lead is attached. Therefore there appears no source for LRTC at the FS boundary.

To demonstrate the enhancement of the LRTC in the ferromagnetic particle with the shifted magnetic vortex we plot in Fig. 2(a) the distribution of the amplitude of the triplet part of the anomalous function $|\hat{f}_{\text{tr}}| = \sqrt{|a_1|^2 + |a_2|^2}$ [see expan-
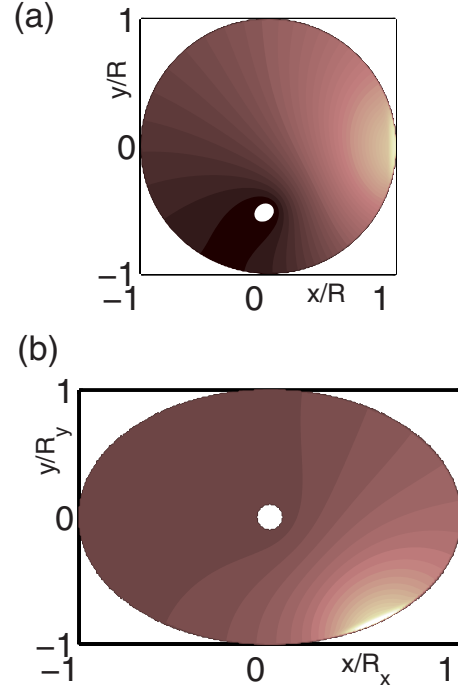

FIG. 2. (Color online) Amplitude of the triplet anomalous function induced due to the proximity effect. The position of magnetic vortex center is marked by the white circle. (a) Shifted magnetic vortex in circular particle; vortex shifting vector is $\mathbf{a} = (0, -R/2)$; and (b) magnetic vortex at the center of elliptical particle with axes ratio $R_x/R_y = 1.5$.

sion (11)]. We choose the position of a superconducting contact $\theta_0 = 0$ and the magnetic vortex shifting vector $\mathbf{a} = (0, a_y)$.

B. Magnetic vortex in elliptical particle

Now let us consider the situation when the magnetic vortex is situated at the center of a particle but the particle itself has elliptical shape. The boundary of the elliptical particle is determined by the equation $(x/R_x)^2 + (y/R_y)^2 = 1$. It is convenient to write the vector normal to the boundary in the polar coordinate frame $\mathbf{n} = n_r\mathbf{r}_0 + n_\theta\boldsymbol{\theta}_0$, where

$$n_r = \frac{R_y^2\cos^2\theta + R_x^2\sin^2\theta}{\sqrt{R_y^4\cos^2\theta + R_x^4\sin^2\theta}},$$

$$n_\theta = \frac{(R_x^2 - R_y^2)\sin(2\theta)}{2\sqrt{R_y^4\cos^2\theta + R_x^4\sin^2\theta}}.$$

Then the short-range modes are given by Eqs. (27)–(29) with $S(\mathbf{r}) = -ie^{i\theta}$ and $(\mathbf{n} \cdot \nabla)S = (n_\theta/r)(dS/d\theta)$, or

$$(\mathbf{n} \cdot \nabla)S = e^{i\theta}\sin(2\theta)\frac{R_x^2 - R_y^2}{2R_xR_y}\sqrt{\frac{R_y^2\cos^2\theta + R_x^2\sin^2\theta}{R_y^4\cos^2\theta + R_x^4\sin^2\theta}}.$$

The boundary condition for the long-range modes [Eq. (43)] then takes form (45) with
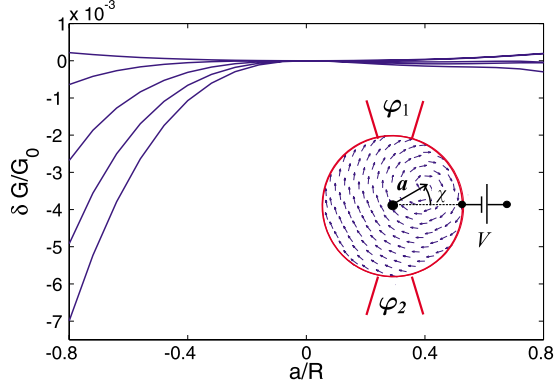
FIG. 3. (Color online) A superconducting phase sensitive correction to the local conductance as a function of the magnetic vortex displacement with respect to the center of a circular ferromagnetic particle (see the inset). Different curves correspond to the angle χ values (from bottom to top): $\chi = 0, \frac{2\pi}{10}, \frac{3\pi}{10}, \frac{4\pi}{10}, \frac{\pi}{2}$.

$$Q(\theta) = \sin(2\theta) \frac{R_x^2 - R_y^2}{2R_x R_y} \sqrt{\frac{R_y^2 \cos^2 \theta + R_x^2 \sin^2 \theta}{R_y^4 \cos^2 \theta + R_x^4 \sin^2 \theta}}.$$

One can see that when the shape of the particle is nearly circular $\delta R = \sqrt{|R_x^2 - R_y^2|} \ll R_x, R_y$ the amplitude of LRTC is determined by the dimensionless factor $(\xi_F / \gamma_0)(\delta R / R_0)$, where $\delta R = \sqrt{|R_x^2 - R_y^2|}$ is a measure of axial anisotropy of the elliptical ferromagnetic nanoparticle and $R_0 = \sqrt{R_x^2 + R_y^2}$.

Since the center of the magnetic vortex is assumed to coincide with the particle center we search the long-range modes in the form of expansion (44) with $\rho = r$ and $\alpha = \theta$. Then we obtain

$$\mathbf{n} \cdot \nabla b_{l0} = \sum_m C_m r^{\sqrt{m^2+1}-1} e^{im\theta} (n_r \sqrt{m^2 + 1} + i n_\theta m).$$

Going along the same lines as in the previous section we find the coefficients C_m numerically and obtain the distribution of the amplitude of the triplet component of the anomalous function shown in Fig. 2(b). We choose the position of the superconducting contact $\theta_0 = \pi / 4$.

V. DISCUSSION

Experimental observation of the proximity effect in FS structures can be done, for example, using Andreev interferometer geometry to measure the modulation of the conductivity of a ferromagnetic sample as a function of the phase difference between the superconducting leads.[11] Therefore it is interesting to investigate the influence of the long-range proximity effect on the transport properties of ferromagnetic nanoparticles. Let us consider a system shown in Fig. 3 (see the inset). We assume that there are two superconducting leads with different phases of the superconducting order parameter $\varphi_{1,2}$ attached at the different points to the circular ferromagnetic nanoparticle. The normal lead measures the conductance of the system. In case of a point junction with normal lead one can use a general relation between a zero-bias tunneling conductance G and a local density of states (LDOS) ν in the ferromagnetic particle at the junction point as follows:

$$G = G_n(\nu / \nu_n), \tag{46}$$

where G_n and ν_n are the point junction conductance and LDOS in the normal state of the ferromagnetic particle. The above expression for the local tunneling conductance is valid only if the voltage drops in the small vicinity of the junction point. This condition can be obtained assuming, for example, that the potential surface barrier is so high that all voltages drop just at the interface between the normal lead and the ferromagnetic particle. But in case of a point junction Eq. (46) can be used even for an ideal interface because the voltage drops at the distance determined by the junction size. Note that it is not so if, for example, a conductance of one-dimensional wire is considered.[12,34] We will assume that the junction size is much smaller than other characteristic lengths and employ expression (46) for the tunneling conductance.

Having found the condensate function $\hat{f}$, we can calculate the LDOS in the ferromagnetic region. The LDOS is given by the general formula[20]

$$\nu = \frac{\nu_n}{4} \mathrm{Re} \, \mathrm{Tr}(\hat{\tau}_3 \hat{\sigma}_0 \check{g}),$$

where $\omega = -i\varepsilon + 0$ and the trace is taken in both the Gor'kov-Nambu and spin spaces. Using the normalization condition $\hat{g}^2 + \hat{f} \hat{f}^+ = 1$ and the smallness of the condensate function, we obtain the correction to the conductance of the point junction as follows:

$$\delta G / G_n = -\frac{1}{2} \mathrm{Re} \, \mathrm{Tr}(\hat{f}\hat{f}^+).$$

The anomalous function $\check{F}$ has the following structure in Gor'kov-Nambu space:

$$\check{F} = \sum_i \hat{f}_i (\sin \varphi_i \hat{\tau}_1 - \cos \varphi_i \hat{\tau}_2),$$

where $\Delta_{1,2} = \Delta_0 \exp(i\varphi_{1,2})$ are the gap functions in the superconducting leads. Therefore,

$$\hat{f} = i e^{-i\varphi_1} \hat{f}_1 + i e^{-i\varphi_2} \hat{f}_2$$

and

$$\hat{f}^+ = i e^{i\varphi_1} \hat{f}_1 + i e^{i\varphi_2} \hat{f}_2.$$

Thus we obtain

$$\delta G / G_n = \frac{1}{2} \mathrm{Re} \, \mathrm{Tr}(\hat{f}_1^2 + \hat{f}_2^2 + 2\hat{f}_1 \hat{f}_2 \cos \varphi), \tag{47}$$

where $\varphi = \varphi_1 - \varphi_2$. Probably the most important for experiments is the conductance correction in Eq. (47) which depends on the phase difference φ due to the interference between the anomalous functions induced by different superconducting leads $\delta G / G_n = \cos \varphi \, \mathrm{Re} \, \mathrm{Tr}(\hat{f}_1 \hat{f}_2)$. In Fig. 3 we show the dependence of the amplitude of conductance modulation $\delta G = G_n \, \mathrm{Re} \, \mathrm{Tr}(\hat{f}_1 \hat{f}_2)$ on the distance of the magnetic vortex center from the center of the ferromagnetic particle. Different curves in this plot correspond to the different

directions of vortex shifting vector **a** (see the sketch of the system considered on the inset in Fig. 3). We normalize the conductance to the following value $G_0 = G_n(\xi_F/\gamma_0)^2$ which is entirely determined by the fixed parameters of the system.

Analyzing Fig. 3 one can see that the strongest effect is achieved by shifting the vortex symmetrically with respect to the superconducting contacts ($\chi = 0$). On the contrary, the effect of conductance modulation is very small in case of the vortex shifting along the line between two superconducting leads ($\chi = \pi/2$, top curve). As we have discussed above, in this case the LRTCs are weak due to the symmetry of the magnetization distribution. A nonzero value of the conductance modulation in this case is caused only by the finite width of the superconducting junctions used in calculations. Furthermore, in Fig. 3 all the curves, except for the top one which corresponds to $\chi = \pi/2$, demonstrate strong asymmetry with respect to the sign of the vortex displacement $\delta G(a) \neq \delta G(-a)$. Such asymmetry is caused by the system geometry since we consider a conductance of only one point junction. As one can see if the magnetic vortex shifts toward the normal contact (positive a in Fig. 3) the conductance modulation appears to be very small compared to the case when the magnetic vortex shifts in the opposite direction (negative a in Fig. 3). This effect can be understood if we recall that the long-range modes are strongly suppressed near the vortex center [see Eq. (33)]. Thus even if the overall amplitude of LRTC is increased with $|a|$, the local value of anomalous function at the junction point is decreased if the magnetic vortex center shifts toward the junction point.

The shift of the magnetic vortex is unambiguously determined by the magnetic field [see Eq. (3)]; therefore, the asymmetry $\delta G(a) \neq \delta G(-a)$ will be revealed in the conductance dependence on the external magnetic field: $\delta G(H) \neq \delta G(-H)$. But in reality one always has two contacts and the total conductance correction is a sum of the contributions from each contact. Thus the resulting behavior of the conductance should depend on the position of the points where superconducting and normal contacts are connected to the ferromagnetic particle. In particular, if the system geometry is symmetric with respect to the spatial inversion the conductance correction will not depend on the sign of vortex shifting a as well as on the sign of the magnetic field $\delta G(H) = \delta G(-H)$.

In Fig. 3 the modulation of conductance is shown not for the entire range of the magnetic vortex displacements from the particle center. The reason is a growing complexity of numerical calculations because when the magnetic vortex center approaches close to the particle boundary one has to take into account too many angular harmonics in expansion (44). We expect further monotonic growth of $|\delta G(a)|$ until $|a| < R$. If the vortex displacement distance becomes larger than the particle radius $|a| > R$, the vortex actually leaves the particle. Such magnetization state often is referred to as "buckle."[28] Further increase in $|a|$ describes in fact a continuous transition to the homogeneously magnetized state. Therefore, the conductance correction should eventually vanish as $|a| \to 0$.

The overall magnitude of the conductance modulations is determined by many factors. One of them is a vortex displacement, which can be regulated by the external magnetic field. Other factors are determined by the geometry of the system, e.g., the width of superconducting leads and the particle size R. Also there is a dimensionless factor ξ_F/γ_0, which depends on the material parameters: ferromagnetic coherence length ξ_F and $\gamma_0 = R_F\sigma_{int}$, where R_F is the resistance per unit area of FS interface and σ_{int} is the conductivity of ferromagnetic.[20] This factor determines the amplitude of the anomalous function within the ferromagnetic region and should be small within our calculation scheme because we consider the linearized Usadel equation. For a particular configuration shown on the inset in Fig. 3 we obtain the maximal amplitude of conductance modulation $\delta G \sim 10^{-2}(\xi_F/\gamma_0)^2 G_n$, where G_n is the unperturbed conductance in the normal state of the particle. To have a better effect in experiment one should try to increase the ratio ξ_F/γ_0. For example this can be obtained by using not very strong ferromagnetic material with relatively large ξ_F, e.g., Cu-Ni alloys,[35] characterized by rather large coherence lengths: $\xi_F \sim 10$ nm. However the magnetic vortex has been observed in rather strong ferromagnets such as C or Pe with $\xi_F \sim 1$ nm. On the other hand, one can try to improve the properties of the superconducting contacts, i.e., to use the contacts with low interface resistance R_F.

VI. CONCLUSION

To summarize we have investigated the proximity effect in the ferromagnetic nanoparticle with nonhomogeneous vortex magnetization distribution. We have derived a general solution both for the short-range components and the long-range triplet components of the anomalous function. Quite generally it is shown that the long-range proximity effect can be realized if the axial symmetry of the magnetization distribution is broken either due to the shifting of magnetic vortex with respect to the particle center or due to the angular anisotropy of the particle shape, which can be, for example, elliptical in real experiments. Also we have considered the superconducting phase-periodic oscillations of the particle conductance in Andreev interferometer geometry, which has been used recently to study the proximity effect in a conical ferromagnet.[11] We have shown that the amplitude of conductance oscillations strongly depends on the direction of external magnetic field which determines the shift of magnetic vortex with respect to the particle center. For a particular case of a circular ferromagnetic particle the conductance oscillations are the largest when the vortex shifting is symmetric with respect to the superconducting contacts position. However, we suppose that the optimal direction of vortex shifting for the observation of the long-range proximity effect should depend on the system geometry, such as particle shape and position of the points where the superconducting and normal contacts are connected to it.

RAS "Quantum Physics of Condensed Matter" and "Strongly correlated electrons in semiconductors, metals, superconductors and magnetic materials", and by "Dynasty" Foundation.

APPENDIX A: DERIVATION OF THE SHORT-RANGE MODES

We search quasiclassical solutions of Eqs. (24)–(26) in the following form:

$$(a_0, b_+, b_-) = \exp(\lambda \mathbf{n} \cdot \mathbf{r})(a_{0q}, b_{+q}, b_{-q}), \tag{A1}$$

where $\mathbf{n}$ is a unit vector, λ is large, and functions a_{0q}, b_{+q}, b_{-q} are slow. Note that in principle the direction of vector $\mathbf{n}$ is arbitrary and should be determined from the boundary conditions. But we assume from the beginning that the spatial scale of the anomalous function variation along the boundary is much larger than $1/|\lambda|$. Thus we can consider vector $\mathbf{n}$ as normal to the boundary of a ferromagnetic. First we need to find λ. Substituting functions in form (A1) into Eqs. (24)–(26) we obtain: $\lambda^4 = -k_h^4$; i.e., $\lambda = (-1)^{1/4}k_h$ which corresponds to the short-range modes and $\lambda = 0$ which we will discuss. For quasiclassical envelopes we obtain the following equations:

$$2\lambda(\mathbf{n}\nabla)a_{0q} + \lambda^2 a_{0q} - i\frac{k_h^2}{2}\operatorname{sgn}(\omega)[S^*(\mathbf{r})b_{+q} + S(\mathbf{r})b_{-q}] = 0, \tag{A2}$$

$$2\lambda(\mathbf{n}\nabla)b_{+q} + \lambda^2 b_{+q} - i\operatorname{sgn}(\omega)k_h^2 S(\mathbf{r})a_{0q} = 0, \tag{A3}$$

$$2\lambda(\mathbf{n}\nabla)b_{-q} + \lambda^2 b_{-q} - i\operatorname{sgn}(\omega)k_h^2 S^*(\mathbf{r})a_{0q} = 0. \tag{A4}$$

Since all λ have large real parts all the solutions decay or grow very fast. We will take into account only those which decay far from the boundary of the ferromagnetic particle. Then we should leave $\lambda_1 = k_h(1+i)/\sqrt{2}$ and $\lambda_2 = k_h(1-i)/\sqrt{2}$. Let us now find the solutions of quasiclassical equations (A2)–(A4). We will use a perturbation method.

Let us at first assume that $a_{0q} = \text{const}$. Then to the zero order,

$$b_{+q} = ia_{0q}\operatorname{sgn}(\omega)\frac{k_h^2}{\lambda^2}S(\mathbf{r}), \tag{A5}$$

$$b_{-q} = ia_{0q}\operatorname{sgn}(\omega)\frac{k_h^2}{\lambda^2}S^*(\mathbf{r}). \tag{A6}$$

Note that we also can assume $a_{0q} = G(\mathbf{r})$, where $G(\mathbf{r})$ is arbitrary but rather slow function. In this case two other coefficients b_{+q} and b_{-q} are proportional to $G(\mathbf{r})$. The condition $(\mathbf{n}\nabla)G \ll |\lambda|$ guarantees that this will not change the structure of eigenmodes. Substituting expressions (A5) and (A6) into Eqs. (A3) and (A4) we obtain the first-order perturbations,

$$\tilde{b}_{+q} = -2ia_{0q}\operatorname{sgn}(\omega)\frac{k_h^2}{\lambda^3}(\mathbf{n}\nabla)S(\mathbf{r}),$$

$$\tilde{b}_{-q} = -2ia_{0q}\operatorname{sgn}(\omega)\frac{k_h^2}{\lambda^3}(\mathbf{n}\nabla)S^*(\mathbf{r}).$$

APPENDIX B: DERIVATION OF THE LONG-RANGE MODES

The long-range modes can be found solving Eqs. (30)–(32) with neglected terms proportional to k_ω^2,

$$\left[\frac{1}{\rho}\frac{\partial}{\partial\rho}\left(\rho\frac{\partial}{\partial\rho}\right) - \frac{M^2}{\rho^2}\right]a_{\rho 0} - \operatorname{sgn}(\omega)\frac{k_h^2}{2}(b_{\rho-} - b_{\rho+}) = 0, \tag{B1}$$

$$\left[\frac{1}{\rho}\frac{\partial}{\partial\rho}\left(\rho\frac{\partial}{\partial\rho}\right) - \frac{(M+1)^2}{\rho^2}\right]b_{\rho+} - \operatorname{sgn}(\omega)k_h^2 a_{\rho 0} = 0, \tag{B2}$$

$$\left[\frac{1}{\rho}\frac{\partial}{\partial\rho}\left(\rho\frac{\partial}{\partial\rho}\right) - \frac{(M-1)^2}{\rho^2}\right]b_{\rho-} + \operatorname{sgn}(\omega)k_h^2 a_{\rho 0} = 0. \tag{B3}$$

It is convenient to rearrange these equations introducing new functions $b_s = b_{\rho+} + b_{\rho-}$ and $b_d = b_{\rho+} - b_{\rho-}$ as follows:

$$\left(\frac{\partial^2}{\partial\rho^2} + \frac{1}{\rho}\frac{\partial}{\partial\rho} - \frac{M^2}{\rho^2}\right)a_{\rho 0} + \operatorname{sgn}(\omega)\frac{k_h^2}{2}b_d = 0, \tag{B4}$$

$$\left(\frac{\partial^2}{\partial\rho^2} + \frac{1}{\rho}\frac{\partial}{\partial\rho} - \frac{M^2+1}{\rho^2}\right)b_s - \frac{2M}{\rho^2}b_d = 0, \tag{B5}$$

$$\left(\frac{\partial^2}{\partial\rho^2} + \frac{1}{\rho}\frac{\partial}{\partial\rho} - \frac{M^2+1}{\rho^2}\right)b_d - \frac{2M}{\rho^2}b_s - 2\operatorname{sgn}(\omega)k_h^2 a_{\rho 0} = 0. \tag{B6}$$

We will find the solutions of these equations as expansion by the orders of the small parameter $(\rho k_h)^{-1}$ assuming that the distance from vortex center is much larger than the ferromagnetic coherence length $\rho \gg \xi_F$. It is easy to see that if $k_h \to \infty$, we obtain that $b_d = 0$ and $a_{\rho 0} = 0$ and

$$\left(\frac{\partial^2}{\partial\rho^2} + \frac{1}{\rho}\frac{\partial}{\partial\rho} - \frac{M^2+1}{\rho^2}\right)b_s = 0. \tag{B7}$$

The solution of this equation is $b_s = B_{s0}\rho^{\sqrt{M^2+1}}$. Then from the Eq. (B6) we get

$$a_{\rho 0} = -\operatorname{sgn}(\omega)\frac{2M}{(k_h\rho)^2},$$

$$b_s = -\operatorname{sgn}(\omega)\frac{2M}{(k_h\rho)^2}\rho^{\sqrt{M^2+1}}B_{s0}.$$

The function b_d is obtained from Eq. (B4) as follows:

$$b_d = -\frac{4M(5 - 4\sqrt{M^2+1})}{(k_h\rho)^4}\rho^{\sqrt{M^2+1}}B_{s0}.$$

Substituting it to Eq. (B5) we obtain the next correction for b_s on the order of $(k_h\rho)^{-4}$ which can be neglected.

[1] A. I. Buzdin, Rev. Mod. Phys. **77**, 935 (2005).

[2] A. I. Larkin and Y. N. Ovchinnikov, Zh. Eksp. Teor. Fiz. **47**, 1136 (1964) [Sov. Phys. JETP **20**, 762 (1965)]; P. Fulde and R. A. Ferrell, Phys. Rev. **135**, A550 (1964).

[3] A. I. Buzdin, Phys. Rev. B **62**, 11377 (2000); T. Kontos, M. Aprili, J. Lesueur, and X. Grison, Phys. Rev. Lett. **86**, 304 (2001).

[4] A. I. Buzdin and M. V. Kuprianov, Pis'ma Zh. Eksp. Teor. Fiz. **52**, 1089 (1990) [JETP Lett. **52**, 487 (1990)]; Z. Radovic, M. Ledvij, L. Dobrosavljevic-Grujic, A. I. Buzdin, and J. R. Clem, Phys. Rev. B **44**, 759 (1991).

[5] M. G. Khusainov and Yu. N. Proshin, Phys. Rev. B **56**, R14283 (1997); L. R. Tagirov, Physica C **307**, 145 (1998).

[6] A. I. Buzdin, L. N. Bulaevskii, and S. V. Panyukov, Pis'ma Zh. Eksp. Teor. Fiz. **35**, 147 (1982) [JETP Lett. **35**, 178 (1982)]; A. I. Buzdin and M. V. Kuprianov, Pis'ma Zh. Eksp. Teor. Fiz. **53**, 308 (1991) [JETP Lett. **53**, 321 (1991)]; V. V. Ryazanov, V. A. Oboznov, A. Yu. Rusanov, A. V. Veretennikov, A. A. Golubov, and J. Aarts, Phys. Rev. Lett. **86**, 2427 (2001).

[7] A. I. Buzdin, A. V. Vedyayev, and N. V. Ryzhanova, Europhys. Lett. **48**, 686 (1999); J. Y. Gu, C.-Y. You, J. S. Jiang, J. Pearson, Ya. B. Bazaliy, and S. D. Bader, Phys. Rev. Lett. **89**, 267001 (2002); L. R. Tagirov, *ibid.* **83**, 2058 (1999).

[8] V. T. Petrashov, V. N. Antonov, S. V. Maksimov, and R. Sh. Shaikhaidarov, Pis'ma Zh. Eksp. Teor. Fiz. **59**, 523 (1994) [JETP Lett. **59**, 551 (1994)]; V. T. Petrashov, I. A. Sosnin, I. Cox, A. Parsons, and C. Troadec, Phys. Rev. Lett. **83**, 3281 (1999).

[9] M. Giroud, H. Courtois, K. Hasselbach, D. Mailly, and B. Pannetier, Phys. Rev. B **58**, R11872 (1998).

[10] J. Aumentado and V. Chandrasekhar, Phys. Rev. B **64**, 054505 (2001).

[11] I. Sosnin, H. Cho, V. T. Petrashov, and A. F. Volkov, Phys. Rev. Lett. **96**, 157002 (2006).

[12] F. S. Bergeret, A. F. Volkov, and K. B. Efetov, Phys. Rev. Lett. **86**, 4096 (2001).

[13] A. F. Volkov, Ya. V. Fominov, and K. B. Efetov, Phys. Rev. B **72**, 184504 (2005).

[14] Ya. V. Fominov, A. F. Volkov, and K. B. Efetov, Phys. Rev. B **75**, 104509 (2007).

[15] A. F. Volkov, A. Anishchanka, and K. B. Efetov, Phys. Rev. B **73**, 104412 (2006).

[16] A. F. Volkov, F. S. Bergeret, and K. B. Efetov, Phys. Rev. Lett. **90**, 117006 (2003).

[17] Ya. V. Fominov, A. A. Golubov, and M. V. Kupriyanov, JETP Lett. **77**, 510 (2003).

[18] V. Braude and Yu. V. Nazarov, Phys. Rev. Lett. **98**, 077003 (2007).

[19] M. Houzet and A. I. Buzdin, Phys. Rev. B **76**, 060504(R) (2007).

[20] F. S. Bergeret, A. V. Volkov, and K. V. Efetov, Rev. Mod. Phys. **77**, 1321 (2005).

[21] R. P. Cowburn, D. K. Koltsov, A. O. Adeyeye, and M. E. Welland, J. Appl. Phys. **87**, 7082 (2000).

[22] A. M. Kosevich, M. P. Voronov, and I. V. Manzhos, Zh. Eksp. Teor. Fiz. **84**, 148 (1983) [Sov. Phys. JETP **57**, 86 (1983)].

[23] Y. Ishii and Y. Nakazawa, J. Appl. Phys. **81**, 1847 (1997).

[24] A. Aharoni, J. Appl. Phys. **68**, 2892 (1990).

[25] S. Tehrani, E. Chen, M. Durlam, M. DeHerrera, J. M. Slaughter, J. Shi, and G. Kerszykowski, J. Appl. Phys. **85**, 5822 (1999).

[26] S. Y. Chou, Proc. IEEE **85**, 652 (1997).

[27] C. A. Ross, H. I. Smith, T. Savas, M. Schattenburg, M. Farhoud, M. Hwang, M. Walsh, M. C. Abraham, and R. J. Ram, J. Vac. Sci. Technol. B **17**, 3168 (1999).

[28] R. P. Cowburn and M. E. Welland, Appl. Phys. Lett. **72**, 2041 (1998).

[29] K. Y. Guslienko and K. L. Metlov, Phys. Rev. B **63**, 100403(R) (2001); K. Y. Guslienko, V. Novosad, Y. Otani, H. Shima, and K. Fukamichi, Appl. Phys. Lett. **78**, 3848 (2001); Phys. Rev. B **65**, 024414 (2001); W. Scholz, K. Y. Guslienko, V. Novosad, D. Suess, T. Schrefl, R. W. Chantrell, and J. Fidler, J. Magn. Magn. Mater. **266**, 155 (2003).

[30] R. P. Cowburn, D. K. Koltsov, A. O. Adeyeye, M. E. Welland, and D. M. Tricker, Phys. Rev. Lett. **83**, 1042 (1999); R. P. Cowburn, A. O. Adeyeye, and M. E. Welland, New J. Phys. **1**, 16 (1999).

[31] N. A. Usov and S. E. Peschany, J. Magn. Magn. Mater. **118**, L290 (1993); Phys. Met. Metallogr. **12**, 13 (1994).

[32] N. B. Kopnin, *Theory of Nonequilibrium Superconductivity* (Oxford University Press, New York, 2001).

[33] D. A. Ivanov and Ya. V. Fominov, Phys. Rev. B **73**, 214524 (2006).

[34] A. F. Volkov and H. Takayanagi, Phys. Rev. B **56**, 11184 (1997).

[35] V. V. Ryazanov, V. A. Oboznov, A. Yu. Rusanov, A. V. Veretennikov, A. A. Golubov, and J. Aarts, Phys. Rev. Lett. **86**, 2427 (2001).